Supporting Information

Lanthanide 9-anthracenate: solution processable emitters for efficient purely NIR emitting host-free OLED

Valentina V. Utochnikova*, Alena S. Kalyakina, Ivan S. Bushmarinov, Andrey A. Vashchenko, Lukasz Marciniak, Anna M. Kaczmarek, Rik Van Deun, Stefan Bräse, *and* Natalia P. Kuzmina

Dr. V.V. Utochnikova, A.S. Kalyakina, D.Sc. Prof. N.P. Kuzmina
Lomonosov Moscow State University, 1/3 Leninskie gory, 119991, Moscow, Russia

Dr. V.V. Utochnikova, Dr. A.A. Vashchenko
Lebedev Physical Institute, 53 Leninskij Prospekt, Moscow, 119991 (Russia)

Dr. I.S. Bushmarinov
A. N. Nesmeyanov Institute of Organoelement Compounds (INEOS), Vavilova St. 28, Moscow, 119991 (Russia)

Dr. A.A. Vashchenko
Moscow Institute of Physics and Technology (State University), Institutskiy per. 9, Dolgoprudny, Moscow Region, 141700 (Russia)

Dr L. Marciniak
Institute of Low Temperature and Structure Research, Polish Academy of Sciences, Wroclaw, (Poland)

Dr. A. M. Kaczmarek, Dr. Prof. R. Van Deun
Ghent University, Krijgslaan 281, building S3, Ghent (Belgium)

A. S. Kalyakina, Prof. S. Bräse
Institute of Organic Chemistry, Karlsruhe Institute of Technology (KIT), Fritz-Haber Weg 6, Karlsruhe, 76131 (Germany); Institute of Toxicology & Genetics, Karlsruhe Institute of Technology (KIT), Kaiserstrasse 12, Karlsruhe, 76131 (Germany)

List of the obtained complexes Ln(ant)$_3$:

№	Ln =	Signals in ^{1}H NMR	Luminescence maxima, nm	Quantum yield, %	Lifetime, ms
1	La	8.55, 8.08, 7.50-7.32	450 (blue)		
2	Pr	9.45, 8.78, 11.55, 7.96-7.75	1050 (NIR)		
3	Nd	8.73, 8.28, 9.17, 9.17	1030 (NIR)		17
4	Eu	8.43, 7.80, 7.13-7.36	450 (blue)		
5	Gd	No signal – too broad	530 (green)	3.8	7.8
6	Tb	11.65, 10.11, 7.55 -8.59	450 (blue)		
7	Dy	14.79, 12.61, 10.45-9.87	450 (blue)		
8	Er	6.89	1500 (NIR)		13
9	Yb	7.12-7.27	980 (NIR)	1.5	52
10	Lu	8.55, 8.08, 7.48-7.43	450 (blue)		

Crystal structure of Ln(ant)$_3$

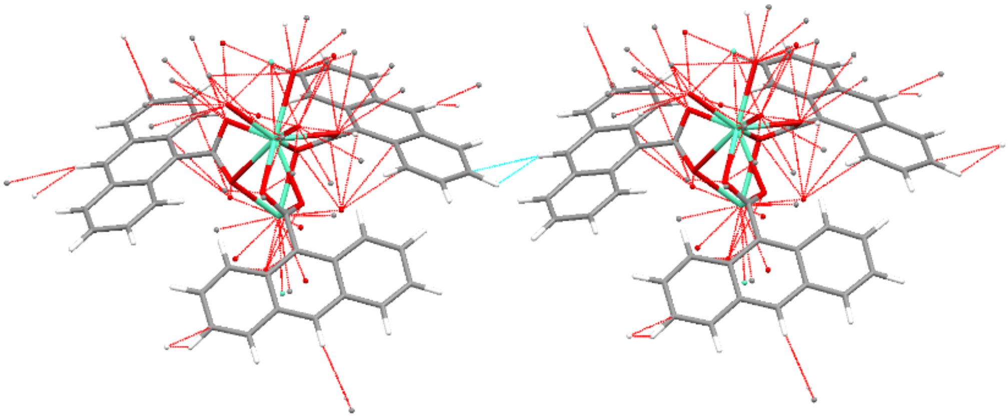

Fig. S1 C-H…H angle in the structure of Eu(**ant**)$_3$

Single crystal structure of Yb(ant)$_3$(DMSO)$_3$·0.16H_2O

Recrystallization of Yb(**ant**)$_3$ from DMSO resulted in formation of single crystals, for which the crystal structure was determined. After the recrystallization the complex crystallized with the solvent molecules, and the composition of the single crystals corresponded to the formula Yb(**ant**)$_3$(DMSO)$_3$·0.16H_2O

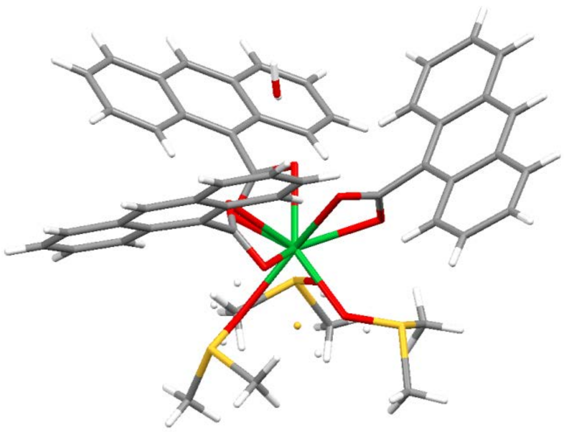

Fig. S2 A molecule in the structure of Yb(**ant**)$_3$(DMSO)$_3$·0.16H_2O

The structure of Yb(**ant**)$_3$(DMSO)$_3$·0.16H_2O consists of monomeric units, where Yb^{3+} ion is coordinated by six oxygen atoms of three bidentate **ant**$^-$ ligands and three oxygen atoms of DMSO molecules, giving the total coordination number of nine (Fig. S2). The Yb-O bonds with **ant**$^-$ ligands have a length of 2.405(2) and 2.415(2) Å and O-Eu-O angles equals to 54.05(2)^o, and Yb-O bond with DMSO length equals to 2.322(1) Å. There is an outersphere water molecule, which takes part in the formation of hydrogen bonds and is bound to the coordinated oxygen atom of carboxylic group of one monomeric unit (d = 2.504 Å) and to the oxygen atoms of carboxylic group and DMSO of another monomeric unit (d = 2.611 and 2.612 Å), thus connecting monomeric units in chains.

SEM and TEM data

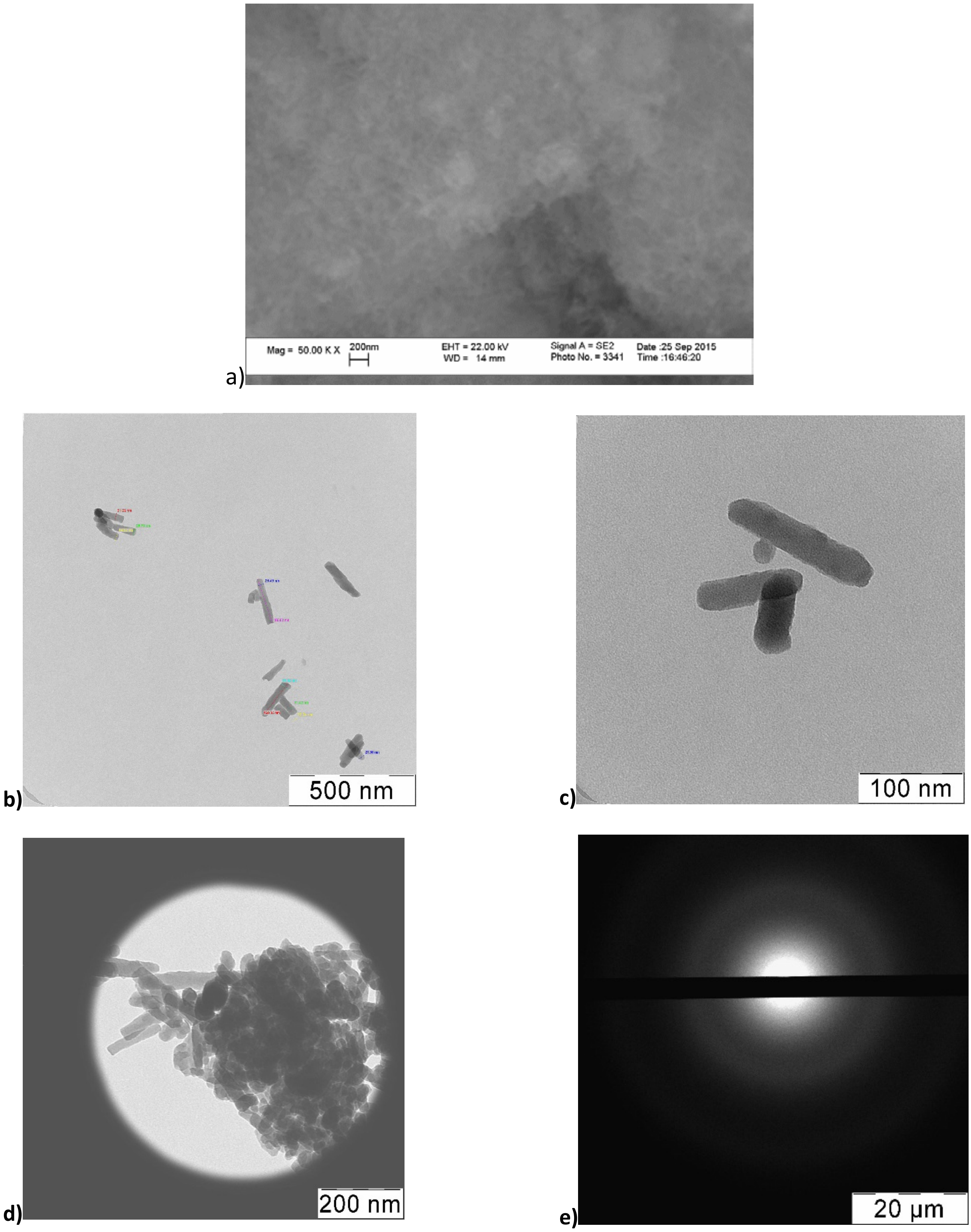

Fig. S3 a) SEM, b-d) TEM images of Tb(**ant**)$_3$, e) an electron diffraction patter from the area shown in d)

EXAFS spectroscopy

Table S1 Several Ln…O, Ln…C and Ln…Ln distances determined from EXAFS data

Atom type	N	Eu	Gd	Tb	Dy	Er	Yb	Lu
O1.1	3	2.37	2.37	2.38	2.36	2.38	2.44	2.39
O2.1	6					2.28	2.25	2.23
C11.1	3	2.94	2.77	2.69	2.79	2.83	2.84	2.82
C11.4	3	3.68	3.38	3.36	3.54	3.29	3.29	3.29
Ln1.1	2	3.72	3.69	3.82	3.82	3.84	3.80	3.80
C5.1	6	4.30	4.01	4.11	4.21	3.90	3.92	3.92
R-factor, %		1.10	0.97	1.16	0.89	1.80	1.02	0.83
R-range		1.6 - 4.5	1.6 - 4.5	1.6 - 4.5	1.6 - 4.5	1.6 - 4.5	1.6 - 4.5	1.6 - 4.5
k-range		2 - 11	2 - 12	2 - 12	2 – 12.5	2 - 13	2 - 13	2 - 14

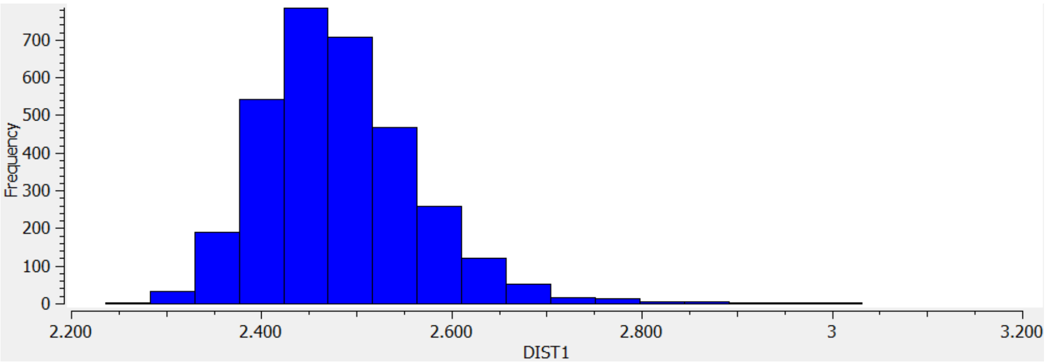

Fig. S4. Distribution of short Ln-O distances for aromatic carboxylates. Average 2.48

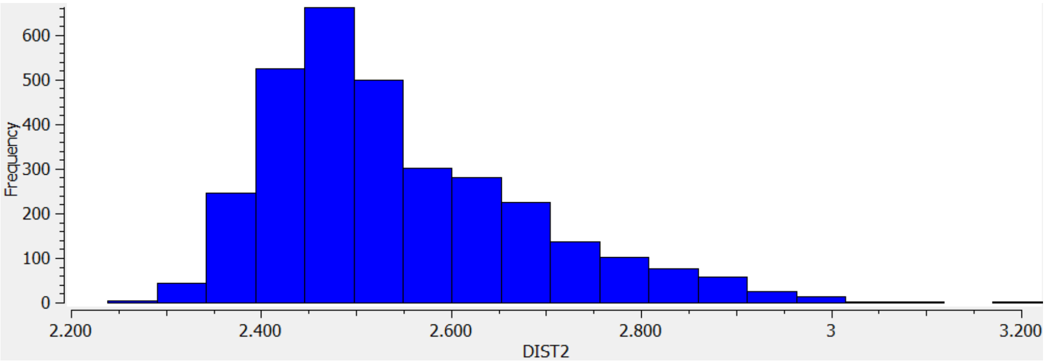

Fig. S5. Distribution of long Ln-O distances for aromatic carboxylates. Average 2.54

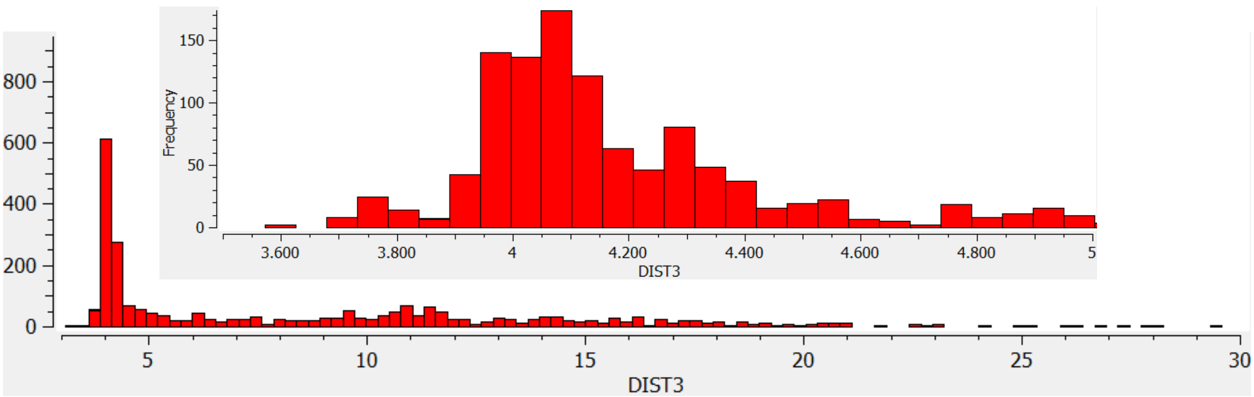

Fig. S6. Distribution of Ln-Ln distances for aromatic carboxylates and (inset) the most interesting range.

NMR spectroscopy
The obtained complexes are only soluble in highly donor solvents as DMSO and DMF, where Ln(**ant**)$_3$ complexes might lose their polymeric structure, stacking and the useful photophysical properties. So, it has been previously shown that from DMFA solution of Er(**ant**)$_3$ a dimeric complex with DMF and water in the first coordination sphere is crystallized [1]; we obtained a monomeric Yb(**ant**)$_3$(DMSO)$_3$·0.16H$_2$O complex upon crystallization from DMSO, where all six ligands are coordinated to ytterbium ion (Fig. S2).
To ensure that in solution **ant**$^-$ is also coordinated to Ln^{3+}, ^{1}H NMR spectroscopy was used. In the presence of paramagnetic ion, such as lanthanide, signals in the NMR spectra are widened and shifted, the additional shift is called pseudocontact shift (PCS). However, as we have found in [2], no shift is observed if the complex completely dissociates in the solution. While if the complex is stable, the PCS values can provide information about complex similar composition in the solution.

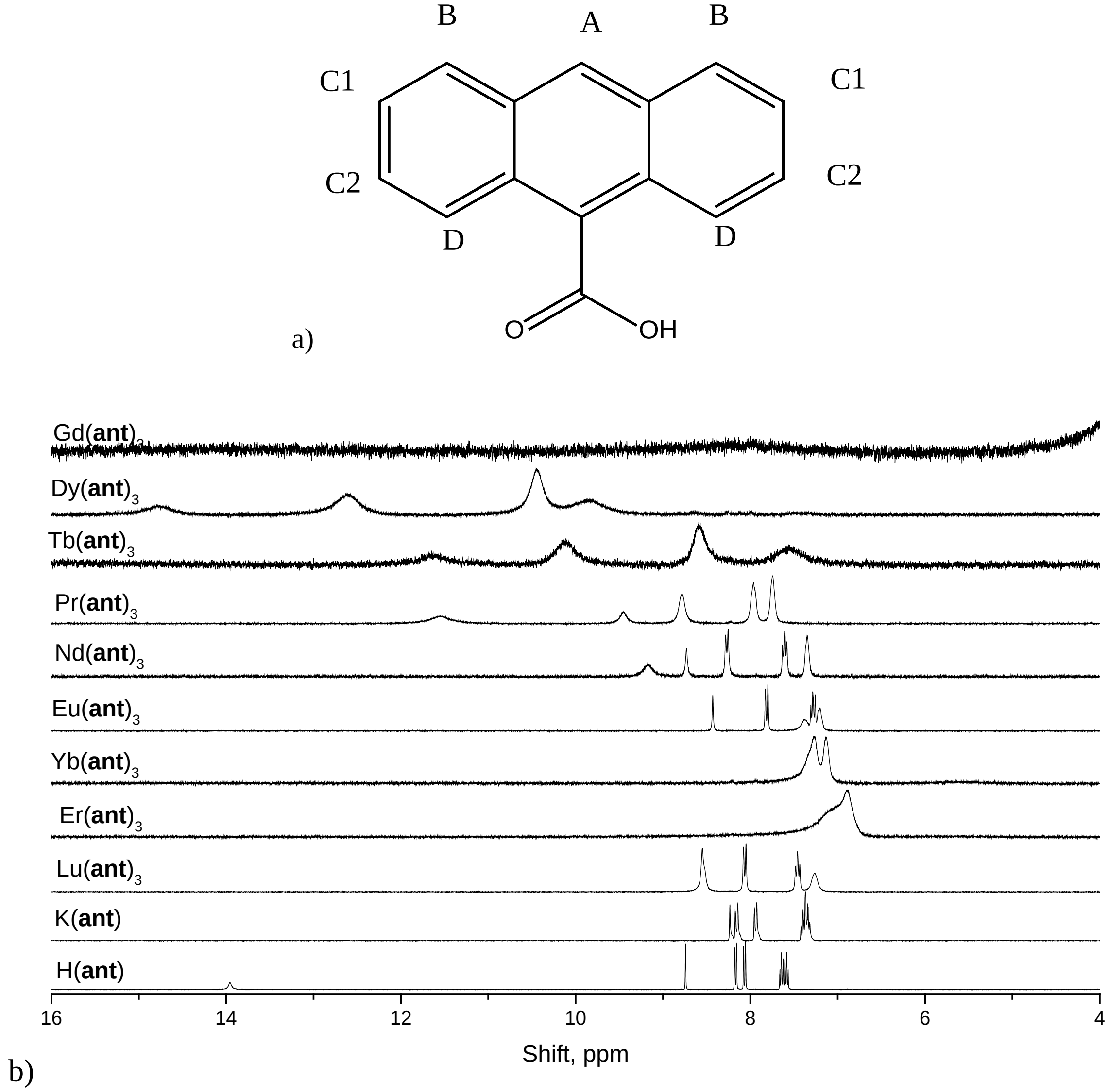

Fig. S7 a) Structural formula of H(**ant**) and b) ^{1}H NMR spectra of H(**ant**), K(**ant**) and Ln(**ant**)$_3$

In the ^{1}H NMR spectra of H**(ant)** five groups of signals, corresponding to the protons A-D (**Fig. S7**) and the acidic proton signal at 13.9 ppm, are present. The same A-D signals, shifted due to deprotonation, are present in the spectra of K(**ant**) and Lu(**ant**)$_3$. The latter spectra are different, which witnesses that they do not belong to free **ant**$^-$ ion, and thus is a proof of at least not complete dissociation of Lu(**ant**)$_3$.

Table S2 Position of the A-D signals in the ^{1}H NMR spectra

	A	B	C1	C2	D
Hant	8.73, s	8.06, 8.03, d	7.65, 7.63, 7.60, 7.57, 7.54, m		8.14, 8.17, d
Kant	8.24, s	7.93, 7.95, d	7.42, 7.40, 7.37, 7.35, 7.32, m		8.1d, 8.18, d
Pr	9.45	7.96,	7.80	8.80	11.55
Nd	8.73	7.63, 7.61, 7.58	7.35	8.28, 8.25	9.17
Eu	8.43	7.83, 7.80	7.38, 7.31, 7.28, 7.26, 7.22, 7.20		
Gd			none		
Tb	7.17	8.62	10.13	11.64	none
Dy	none	9.87	10.43	12.61	14.79
Er			6.89		
Yb			7.28, 7.14, 5.71		
Lu	8.55*	8.08, 8.05, d	7.28	7.48, 7.46, 7.43	8.55*

The ^{1}H NMR spectra of other Ln(**ant**)$_3$ complexes in DMSO-d^6 demonstrated both signal PCS and widening due to paramagnetic relaxation enhancement (PRE) (Fig. S7). In the spectrum of Gd(**ant**)$_3$ the widening is so remarkable that no signals could be detected; the widest signals were detected in the spectra of Dy(**ant**)$_3$ and Tb(**ant**)$_3$ due to the highest PRE radius [3].
Signals in the spectra of Er(**ant**)$_3$ and Yb(**ant**)$_3$ shifted to the weaker field, leading to their overlap. In contrast, the upfield shift in case of signals in the spectra of Ln(**ant**)$_3$ (Ln = Nd, Pr, Tb, Dy) allows to distinguish between D1 and D2 protons, since D2 protons are more shifted and widened, being nearer to the COO-group and thus to the lanthanide ion.

Bleaney theory. The appearance of PCS and widening is another proof that the complex does at least not completely dissociate in DMSO-d^6 solution. The similarity of the local structure of these complexes in solution can be also determined using the Bleaney's equation. Provided that the molecular geometry is independent of the lanthanide ion, the full chemical shift Δ depends linearly on the D-factor [4] – the characteristic of the lanthanide:

$$\Delta = D \cdot G_i + C \qquad (1)$$

Here C is a constant; full shift $\Delta = \delta_c + \delta_d$, where δ_c – contact chemical shift and δ_d – dipolar chemical shift; and $\delta_d = D \cdot G_i$, where G_i is the geometrical function of the ligand, which is constant for isomorphous compounds.
The positions of the ^{1}H NMR signals and the Δ(D) dependencies for each proton are given in the **Table S2**. All these dependencies appeared to be linear, proving the identical local structure in solution of the lanthanide anthracenates.

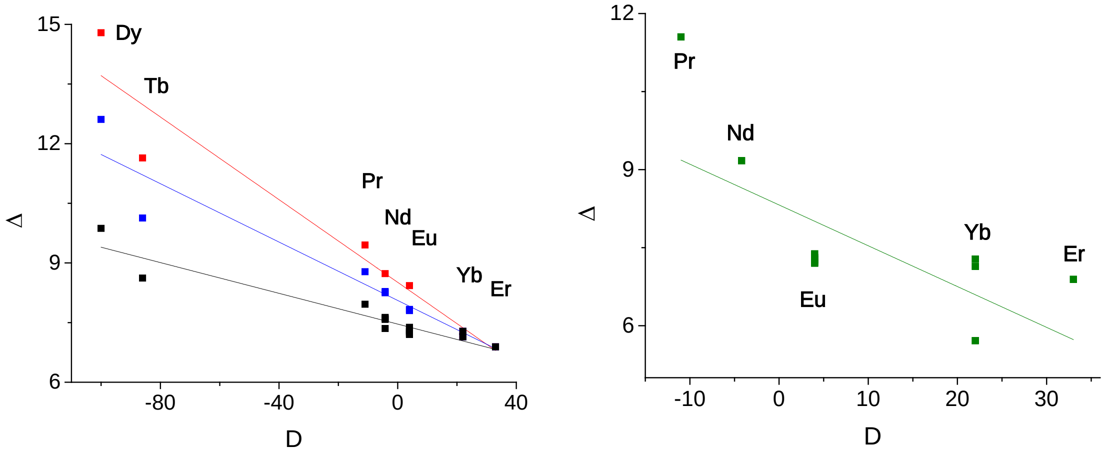

Fig. S8 The chemical shift dependency on D for proton signals of Ln(**ant**)$_3$: a) A(red), B (blue), D (black) and b) C (green)

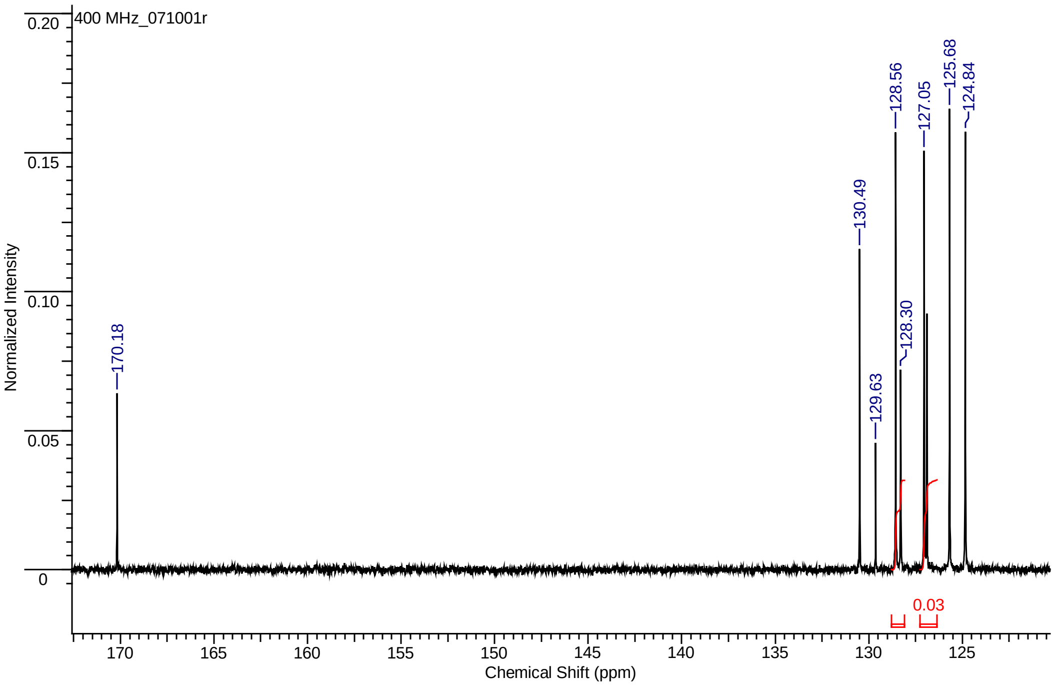

Fig. S9. ^{13}C NMR spectrum of H(**ant**)

Photophysical data

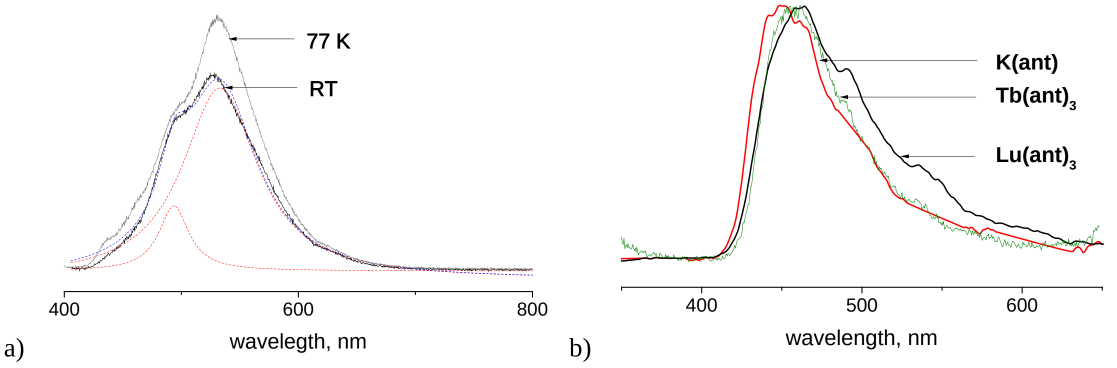

Fig. S10 Steady-state luminescence spectra of a) Gd(**ant**)$_3$ at 77K and room temperature; RT luminescence band is deconvoluted, b) K(**ant**), Tb(**ant**)$_3$ and Lu(**ant**)$_3$ at room temperature

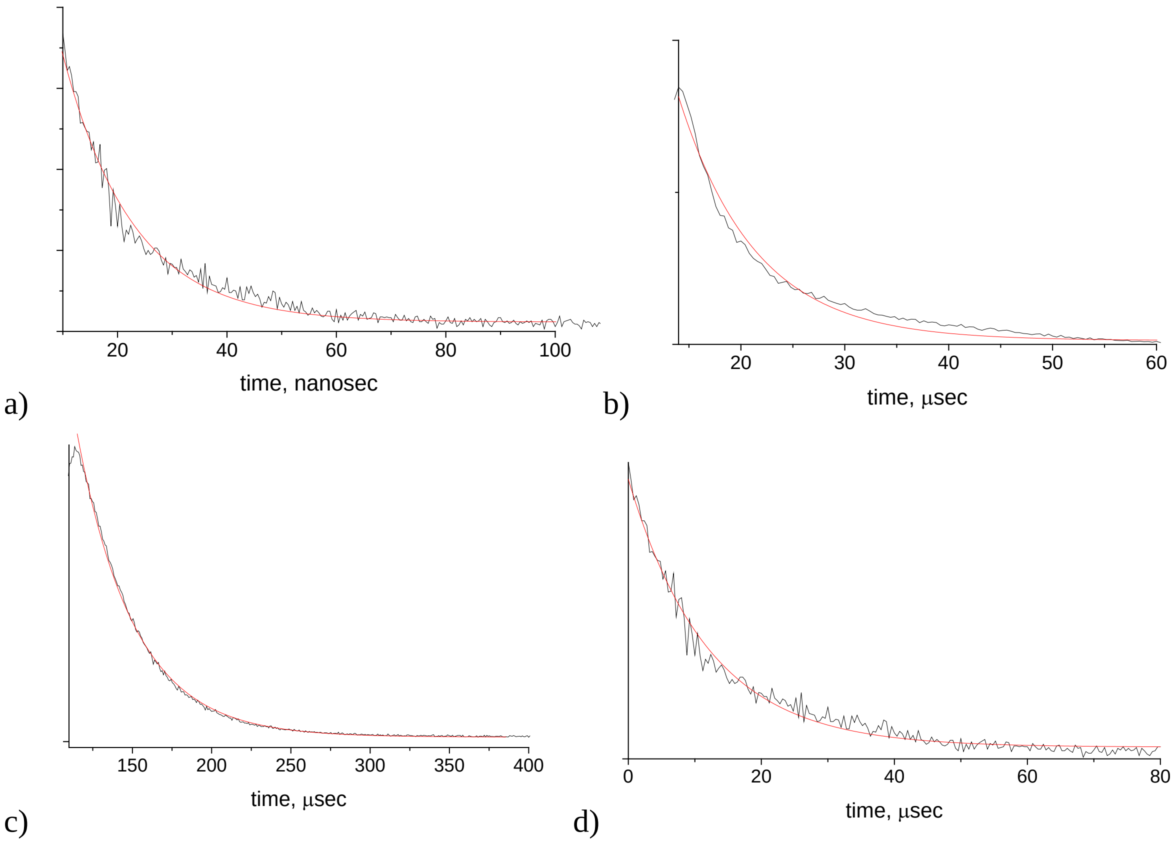

Fig. S11 Luminescence decay curves of a) Nd(**ant**)$_3$, b) Gd(**ant**)$_3$, c) Yb(**ant**)$_3$ and d) Er(**ant**)$_3$

Electronic spectra

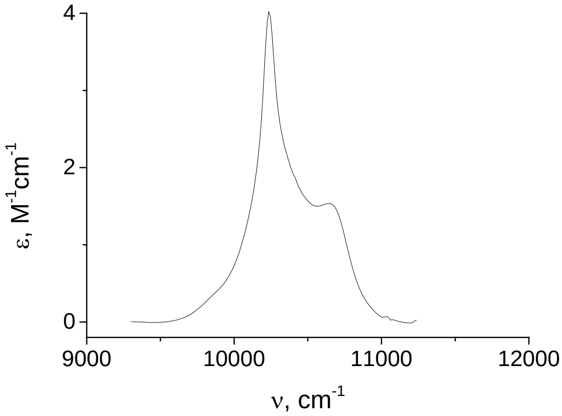

Fig. S12. Absorption spectra in the range of the Yb^{III} $^2F_{5/2}$←$^2F_{7/2}$ transition for Yb(**ant**)$_3$ (18 mM, DMSO, 298 K)

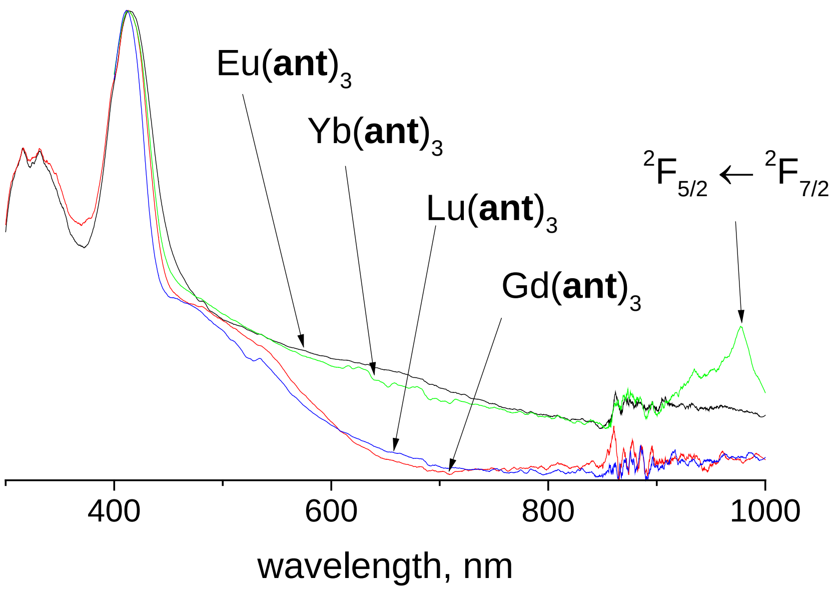

Fig. S13. Diffuse reflection spectra of Ln(**ant**)$_3$ (Ln=Eu, Gd, Yb, Lu)

TGA data

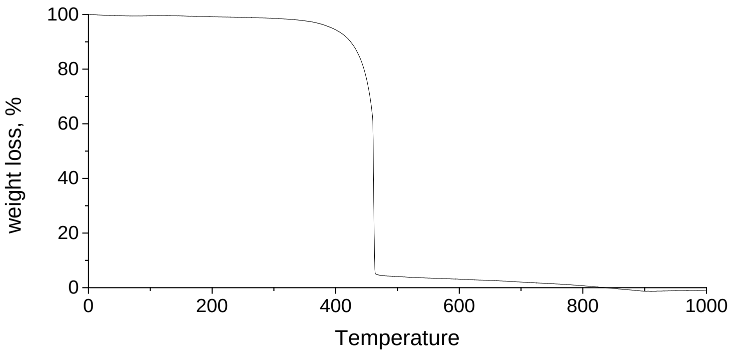

Fig. S14. TGA curve of Yb(**ant**)$_3$

OLED fabrication

Though the “HOMO” and “LUMO” energies are not defined for a polymeric material, and the studied compounds are polymers $[Ln(ant)_3]_n$. For an initial approximation of the HOMO and LUMO energies of the ligand anion, we performed a calculation of Na(ant) in isolated state at OLYP/L2[1] level in Priroda[2], resulting in values of -4.26662 and -2.46951 eV respectively.

Though ytterbium has low magnetic moment, phosphorescence and not fluorescence band is present in the electroluminescence spectrum of Yb(**ant**)$_3$. It is probably due to the peculiarities of the excited state formation at electroexcitation, where 75% of the generated excited states are triplet. The EL spectrum did not significantly change with variation of the operating bias voltages from 5 to 12V.

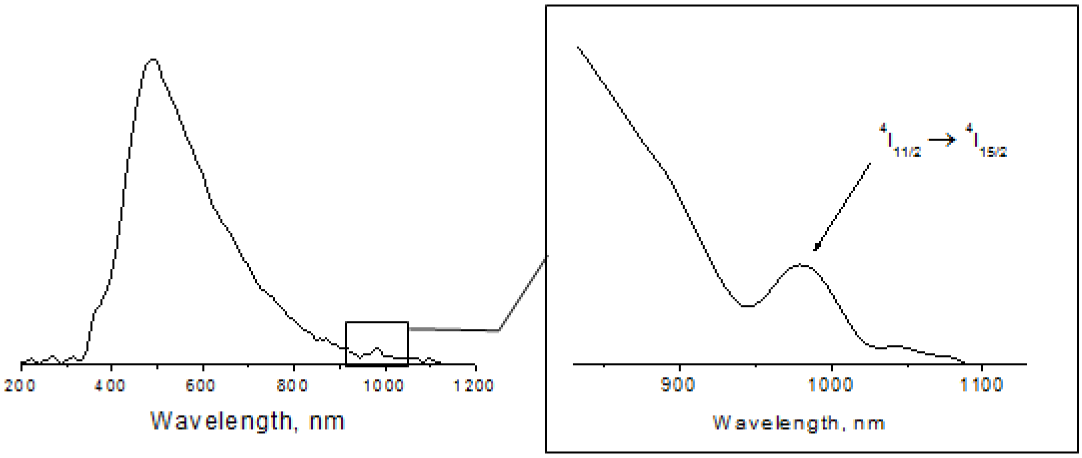

Fig. S15. Electroluminescence spectra of the device ITO/PEDOT:PSS/Er(**ant**)$_3$/TAZ/Al

Literature

1. Kusrini E. et al. Synthesis and structure of dimeric anthracene-9-carboxylato bridged dinuclear erbium(III) complex, [Er2(9-AC)6(DMF)2(H2O)2] // Spectrochim. Acta Part A Mol. Biomol. Spectrosc. 2009. Vol. 72, № 4. P. 884–889.
2. Kalyakina A.S. et al. Highly Luminescent, Water-Soluble Lanthanide Fluorobenzoates: Syntheses, Structures and Photophysics, Part I: Lanthanide Pentafluorobenzoates // Chem. - A Eur. J. 2016. Vol. 21, № 49. P. 17921–17932.
3. Otting G. Protein NMR using paramagnetic ions. // Annu. Rev. Biophys. 2010. Vol. 39. P. 387–405.
4. Bleaney B. Nuclear magnetic resonance shifts in solution due to lanthanide ions // J. Magn. Reson. 1972. Vol. 8. P. 91–100.